Fixture Failure Diagnosis for Sheet Metal Assembly with Consideration of Measurement Noise

D. Ceglarek
Department of Mechanical Engineering and Applied Mechanics
darek@engin.umich.edu

J. Shi
Department of Industrial and Operations Engineering
shihang@engin.umich.edu

The University of Michigan, Ann Arbor, MI 48109

This paper expands previously developed assembly fixture fault diagnosis methodology (Ceglarek and Shi, 1996) by considering the impact of measurement noise on the diagnostic results. The proposed solution provides a new analytical tool to address the diagnosability issue during the assembly process design stage. An evaluation of fault diagnosis index as a function of noise, fixture geometry, and sensor location is presented. The index is derived from the general class of covariance matrices describing tooling faults. Simulation based on the real fixture is presented to illustrate the proposed method.

1 Introduction

Failures of assembly fixture critically affect the dimensions of an automobile. In automotive body assembly, dimensional accuracy is one of the most important quality and productivity factors. Studies on the assembly of a sport utility vehicle showed that 72 percent of all dimensional failures were attributable to fixtures (Ceglarek and Shi, 1995).

Ceglarek and Shi (1996) developed a methodology of fixture failure diagnosis using Principal Components Analysis (PCA) based on the in-line measurement data of critical points on the assemblies and geometrical models of fixtures. This methodology isolates the root causes of a dimensional failure in the fixtures based on the: (1) geometrical model of the fixture failure patterns, (2) the fault variation pattern obtained from in-line multisensor data, and (3) pattern recognition of the fault by mapping fault variation pattern to the fixture failure model.

The fixture diagnostic methodology provides an analytical tool to control the assembly process. However, effective utilization of this method is still a challenge. These challenges can be summarized as follows:

(1) *Sensor synthesis in the dimensional analysis considering measurement noise:* Variation patterns of a part's orientation and position can be identified by dimensional sensors (Tlusty and Andrews, 1983) and modeled using geometrical information about fixture and sensor readings (Ceglarek and Shi, 1996). However, no analysis including measurement noise in modeling variation patterns and PCA analysis has been conducted. This omission is especially important because general measurement data captured on the plant floor are affected by noise.

(2) *Integration of error analysis, advanced statistics, and engineering knowledge for root cause isolation:* Pure statistical methods, without knowledge about the product and process, are not sufficient to identify the root cause of a fault (Schwarz and Lu, 1992). Integration of engineering knowledge with statistics is especially important during dimensional diagnosis of a multi-fixture system such as an autobody assembly (Hu and Wu, 1992; Ceglarek et al., 1994). However, industrial utilization of the diagnosis method requires consideration of the impact of noise on the diagnostic results. Currently, no assembly fixture model and PCA for diagnostic purposes takes the measurement noise into account.

This paper tries to resolve the above mentioned challenges. It expands upon the earlier developed fixture fault diagnostic methodology (Ceglarek and Shi, 1996) by considering the impact of measurement noise on diagnostic results. The developed approach evaluates the diagnosability of the fixture diagnosis method by estimating the error of fault variation patterns caused by additive noise. An evaluation of fault diagnosis as a function of noise, fixture geometry, and sensor location is presented. The proposed solution provides a new analytical tool to address the diagnosability issue during the design stage of assembly process.

The paper is divided into five sections. Section 2 briefly reviews the fixture diagnosis methodology. Section 3 derives relations of fixture geometry with: (1) measurement data (covariance matrix), and (2) fault variation pattern (eigenvalue-eigenvector pair) affected by additive measurement noise. Section 4 presents the fixture failure diagnosis with additive uncorrelated noise. Finally, Section 5 draws the conclusions and summarizes the conducted study.

2 Review of Fixture Failure Diagnosis

This section briefly reviews the fixture failure diagnostics essential for our study on impact of measurement data noise.

The characteristics of a correctly functioning fixture, including, locating and clamping stability, deterministic part location, and total restraint (Chou et al., 1989), are directly realized through the tooling elements (TE) of a fixture, i.e., locating pins (P) and NC blocks (noted as C = NC locator + clamp)[1] (Fig. 1). We assume that P's and C's have primary responsibility for the correct functioning of a fixture, and therefore, for the level of product dimensional variation. TE faults are any tooling discrepancies that cause part mislocation. TE faults can be caused by locator wear, inclusions on the locating surface of locators, or clamps that do not properly force the part/subassembly against the locators (Ceglarek and Shi, 1996). These faults manifest themselves in the measurement data of the final product in the form of different variation patterns such as, mean shift, variance change, spikes, cycle, mixture, and so on. The concept of tooling element fault allows us to deal with the dynamic nature of the assembly process such as process maintainability or dimensional variation reduction.

The methodology for diagnosing fixture related dimensional faults in the assembly process is based on a three step procedure (Fig. 2): (a) deriving the variation pattern model based on the fixture layout

Contributed by the Manufacturing Engineering Division for publication in the JOURNAL OF MANUFACTURING SCIENCE AND ENGINEERING. Manuscript received Dec. 1997; revised April 1999. Associate Technical Editor: E. DeMeter.

[1] NC blocks/NC locators describe planar locator(s) perpendicular to the intended constraining direction. The terms "NC block" or "NC locator" are used commonly in automotive industry, and was historically derived from the term NC-Numerically Controlled, as all locators supposed to be machined by NC machine tools.

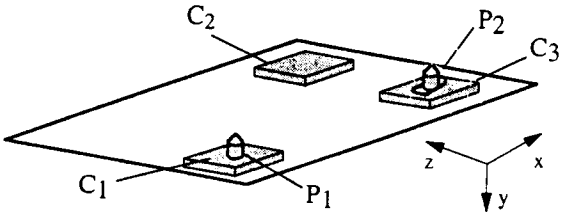

a) A *3-2-1* fixture layout

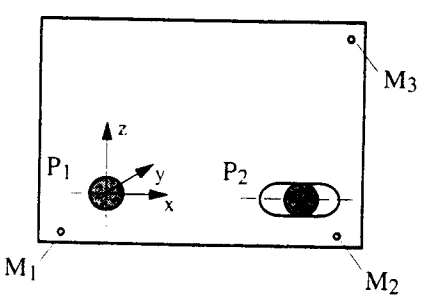

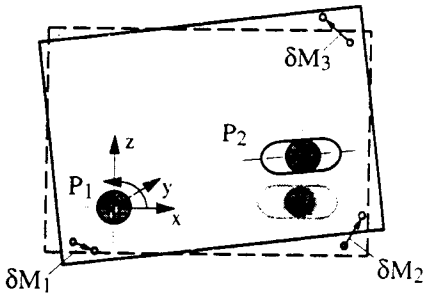

(b) Part locators and measurements (M_i) layout (c) Manifestation of fixture locator P_2 failure

Fig. 1 A 3-2-1 fixture layout and an example of fault manifestation

geometry (CAD data), (b) determining the variation pattern of the unknown fault based on the measurement data, and (c) mapping the fixture fault based on the minimum distance classifier.

Fixture Layout and Hypothesis of the Fixture Faults. The most common fixture layout is 3-2-1 principle, which locates part by three groups of locators (TEs), laid out in two orthogonal planes. As shown in Fig. 1 these three groups usually include: (1) a four-way pin P_1 to precisely position the part in two directions on the first plane, (2) a two-way pin P_2 or NC block to locate the part in one direction laid in the first plane, and (3) all remaining NC locators (C_1, C_2, and C_3) to locate the part in the second plane. Therefore, a six fault system constitutes a complete set of potential root causes of the dimensional faults in the fixture.

Each TE controls a part in the defined direction-control axis. For example, the Z axis is the control axis of the locating pin P_2 (Fig. 1). Furthermore, for each tooling element (TE_i) can be defined a complement tooling element (CTE) in the given control axis Ξ, as any other tooling element (TE) of the fixture, which controls the part in the same Ξ axis, except the tooling element TE_i. Dimensional faults caused by TE failures manifest themselves in specific pre-determined ways: (1) translation along the Ξ axis; if the number of CTEs, $n_{CTE} = 0$, for example, failure of P_1 in X axis, (Figs. 1(*a*) and 3); (2) rotation along the axis defined by one complement tooling element, if the number of CTEs, $n_{CTE} = 1$ (failure of P_2; Figs. 1(*a, c*) and 3); and (3) rotation along the axis defined by two complement tooling elements, if the number of complement tooling elements to TE, $n_{CTE} = 2$ (failure of C; Figs. 1(*a*) and 3).

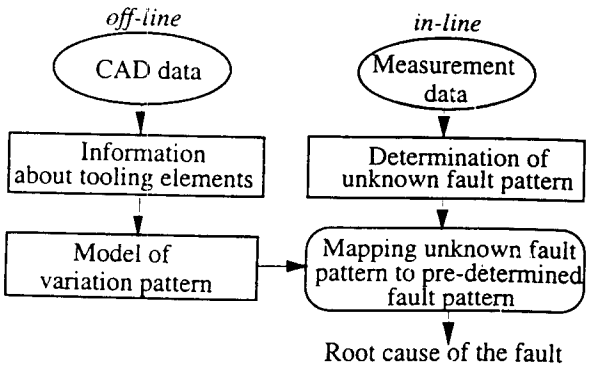

Fig. 2 Outline of the fixture failure diagnosis method

Diagnostic Model of Variation Pattern for 3-2-1 Layout Fixture. The manifestations of the TE faults are represented by sensors M_i (M_{ix}, M_{iy}, M_{iz}) and their standard deviations σ_i (σ_{ix}, σ_{iy}, σ_{iz}), $i = 1, 2, 3$ (Fig. 1(*b*)). The magnitude of dimensional variation captured by the sensor i (σ_i) depends on the severity of the fault described by the standard deviation of the TE, σ_{TE}^k, as well as on the geometrical relations between the location of the sensors and the TEs. These relations can be summarized as (Ceglarek and Shi, 1996): $\sigma_{TE}^k = k_i\sigma_i$, where $k_i = f_k(n_{CTE}, d(TE, CTE), d(CTE, M_i))$, and $d(CTE, TE)$, $d(CTE, M_i)$ are distances between TE–CTE, and CTE–M_i respectively. $f(\,)$ is a function defined in Ceglarek and Shi (1996).

The diagnostic model of the 3-2-1 fixture layout describes the part variation pattern in terms of the TE's and the measurement layout. A total of 9 variables χ_j, $i = 1, 9$ (3 sensors, each measuring 3 axes) are used to describe the 3-2-1 fixture. The model of the variation pattern for the 3-2-1 fixture is described by diagnostic matrix $\mathbf{D} = (\mathbf{d}(1), \ldots, \mathbf{d}(6))$, where $\mathbf{d}(i) = (d_{1i}, \ldots, d_{ni})^T$ is a diagnostic vector describing a type-i fault (Fig. 3), with n (=9) entries corresponding to the measured variables χ_j: $d_{ji} = \sigma_{\chi_j}/\sigma$, $j = 1, \ldots, n$, where σ_{χ_j} is the standard deviation of variable χ_j, and $\sigma = \sqrt{\sum_{j=1}^{n} \sigma_{\chi_j}^2}$.

A major advantage of the proposed model is that the fixture faults can be determined based on the CAD data available during tooling design, before the start of production.

Statistical Representation of a Variation Pattern. The variation pattern caused by an unknown fault is described by multisensor data using a multivariate statistical approach, Principal Component Analysis (PCA) (Jolliffe, 1986). PCA describes a variation pattern by finding $p \leq n$ linear transformations of n variables. Each variable represents measurement data from one of three sensors (M_1, M_2 and M_3) in one axis (X, Y or Z), i.e., $n =$

Fault	Fault of P_1	Fault of P_1	Fault of P_2	Fault of C_1	Fault of C_2	Fault of C_3
Fault type	Type-1	Type-2	Type-3	Type-4	Type-5	Type-6
Fault manifestation	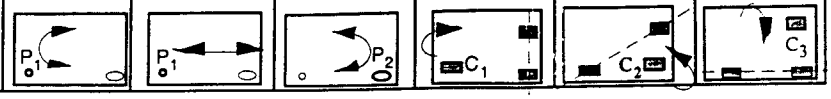					

Fig. 3 Fault manifestation of variation pattern for 3-2-1 layout fixture

9. Eigenvectors $\mathbf{a}_i^T = (a_{i1}, \ldots, a_{i9})$ represent variation patterns. Geometrically, the first eigenvector points in the direction of the greatest variability in the data, and the orthogonal projection of the data onto this eigenvector is the first eigenvalue.

The dominant eigenvector ($\mathbf{a}_1$) of the variation pattern described by the TE failure and obtained from the measurement data, is equal to the diagnostic vector $\{\mathbf{d}(i)\}$ describing the failure of this TE and obtained based on the fixture geometry.

Fault Mapping Procedure. The fault mapping procedure is based on a minimum distance classifier designed for each fixture based on the model of the variation patterns. The mapping procedure minimizes the distance between one of the diagnostic vectors $\mathbf{d}(i)$ and the variation pattern of the unknown fault described by eigenvector $\mathbf{a}$, defined as discriminant function (Ceglarek and Shi, 1996):

$$g_i(\mathbf{a}) = \{\mathbf{d}^T(i)\mathbf{a} - 0.5\|\mathbf{d}(i)\|^2\}, \quad i = 1, 2, 3. \tag{1}$$

Evaluation of the fault mapping procedure is based on index η. η is the relative distance between the unknown fault pattern obtained from the principal components ($\mathbf{a}$), and the closest predetermined type-i fault pattern ($\mathbf{d}(i)$):

$$\eta = 2\|g(\mathbf{a}) - g(\mathbf{d}(i))\| \cdot 100\% \tag{2}$$

3 Impact of the Additive Uncorrelated Noise on the Estimation of Fault Variation Pattern

This section presents a method for estimating the variation pattern error caused by the noise of measurement data.

The diagnostic of fixture is conducted based on the measurement data from multisensors. Each sensor measures different points located on the measured stamped part/subassembly. Additionally, each sensor is an independent device, which measures stamped parts/subassemblies independent from each other. Furthermore, it is assumed that all measurement gages, before they are allowed to be used for taking measurements during production, need to pass repeatability and reproducibility (R&R) test (Down et al., 1995). By passing both tests the measurement gages should be "in statistical control" with all data being independent from each other. This mean that the variation in the measurement system is due to common causes only and not due to special causes (statistical stability). Therefore, we assumed that the measurement noise generated by each sensor could be considered as uncorrelated. The problem of noise, however, is highly nontrivial both from the conceptual as well as from the mathematical points of view. Noise may mean one or all of these factors: inaccuracy of the model, measurement errors, unknown effects, nonlinearities, any casual or random factors which cannot be modeled and of which no further information is available, etc.

The impact of noise on the variation pattern can be estimated through the following two steps: (1) derive the relation between the diagnostic model of fault variation patterns obtained from the (i) fixture layout geometry and (ii) the covariance matrix of measurement data (Section 3.1), and (2) derive the error of the eigenvalue-eigenvector pair (statistical representation of fault variation pattern) caused by additive uncorrelated noise (Section 3.2). The notation used in this section is presented as follows.

Let $\chi_1^o, \chi_2^o, \ldots, \chi_n^o$ denote the vectors of the true values (without noise) of those items measured by sensors $1, \ldots, n$ respectively, where $\chi_i^o = [x_{i1}^o, x_{i2}^o, \ldots, x_{iN}^o]$ is a sample of N measurements of the true values that would be measured by the i-th sensor without noise present. There is also the assumption that $\chi_1^o, \chi_2^o, \ldots, \chi_n^o$ constitutes a random sample, and $\chi_i^o \sim N(0, \sigma_i^2)$, $i = 1, \ldots, n$. Furthermore, let $\chi_1, \chi_2, \ldots, \chi_n$ represent the real values measured by sensors $1, \ldots, n$, where $\chi_i = [x_{i1}, x_{i2}, \ldots, x_{iN}]$ is a sample of N measurements of the i-th sensor. The difference between the measurements with and without noise are error vectors $\mathbf{e}_1, \mathbf{e}_2, \ldots, \mathbf{e}_n$, where $\mathbf{e}_i = [e_{i1}, e_{i2}, \ldots, e_{iN}]$ is an i-th error vector with an individual error for each measurement. In light of the previous definitions, we can write:

$$\chi_i = \chi_i^o + \mathbf{e}_i \tag{3}$$

The elements of the error vectors $\mathbf{e}_i$ follow normal distributions with zero means, i.e., $e_i \sim N(0, \sigma_{e_i}^2)$, $i = 1, \ldots, N$. In this section it is assumed that $\sigma_{e_i}^2 \equiv \sigma_e^2 \ \forall i$. A similar measurement error model was investigated by Grubbs (1948) and Thompson (1963). See Anderson (1965) for a general background on the subject. Based on the results obtained by Thompson (1963), the covariance matrix of the measurement error model expressed by Eq. (2) is equal to:

$$\Sigma = \Sigma^o + \sigma_e^2\mathbf{I} \tag{4}$$

where $\mathbf{I}$, Σ, and Σ^o are identity matrix, covariance matrix of the data with noise, and covariance matrix of the data without noise, respectively.

3.1 Relation between Fixture Geometry and Covariance Matrix. This section investigates relations between fixture geometry and the covariance matrix Σ^o, assuming the occurrence of a single fault without any measurement noise. Let us define the elements of the covariance matrix as:

$\sigma_{ij} = E[(\chi_i - \bar{\chi}_i)(\chi_j - \bar{\chi}_j)]$ or as sample covariance

$$\sigma_{ij} = 1/(N-1)\sum_{k=1}^{N}(x_{ik} - \bar{x}_i)(x_{jk} - \bar{x}_j) \tag{5}$$

where x_{ik} is a k-th measurement of the i-th sensor.

Ceglarek and Shi (1996) stated that the magnitude of the dimensional variation captured by sensors depends on: (1) the severity of the fault (σ_{TE}^F), and (2) the geometrical relations between the sensors and location of TE's. This statement can be generalized by deriving relations between the elements of the covariance matrix and the fixture geometry.

Theorem 1. The relations between fixture geometry and covariance matrix, during failure of the tooling element TE, are described by measurement data without noise from sensors M_1, M_2, M_3 as follows:

(1) when the number of complement tooling elements $n_{CTE} = 0$

$$(\sigma_{TE}^F)^2 = \sigma_{ij} \quad \forall i, j \tag{6}$$

(2) when the number of complement tooling elements $n_{CTE} = 1$

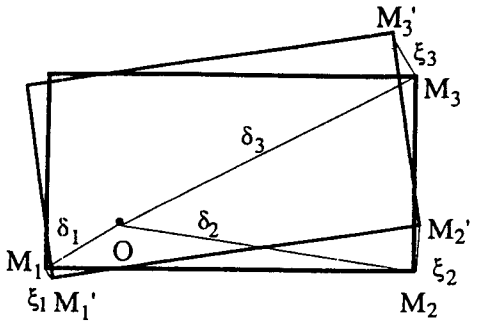

Fig. 4 Geometrical relations during rotation of a rigid part

$$\sigma_{ij} = \frac{d(\text{CTE}, M_i)d(\text{CTE}, M_j)}{d^2(\text{TE}, \text{CTE})}(\sigma_{\text{TE}}^F)^2 \quad \forall\, i, j \quad (7)$$

where $d(a, b)$ is the Euclidean distance between points a and b.

(3) when the number of complement tooling elements $n_{\text{CTE}} = 2$

$$\sigma_{ij} = \frac{d(\text{CTE}_{12}, M_i)d(\text{CTE}_{12}, M_j)}{d^2(\text{TE}, \text{CTE}_{12})}(\sigma_{\text{TE}}^F)^2 \quad \forall\, i, j \quad (8)$$

where CTE_{12} is the axis between complement tooling elements 1 and 2.

Proof. The proof for Eq. (7) is conducted. Equations (6) and (8) can be proven following the same procedure. Eq. (7) presents the case when $n_{\text{CTE}} = 1$, which describes the fault that causes the variation pattern represented as a rotation around the CTE. Let M_1, M_2, M_3 and M_1', M_2', M_3', be the points located on the component before and after rotation of that component respectively (Figs. 1 and 4). And let δ_1, δ_2, δ_3 describe the distance of each of the M_1, M_2, M_3 points from the center of rotation O. Simultaneously ξ_i is the distance between points M_i and M_i' $(i = 1, 2, 3)$.

First, observe that in general $\xi_1/\delta_1 = \xi_2/\delta_2 = \xi_3/\delta_3$, holds for rotation of the part, so this relation can be rearranged as:

$$\xi_{i+1} = (\delta_{i+1}/\delta_i)\xi_i = \kappa_i\xi_i \quad \text{for } i = 1, 2 \quad (9)$$

where $\kappa_i = \delta_{i+1}/\delta_i$ is a constant. After rearranging Eq. (9) and substituting $\xi_i = x_{ik}$ for the k-th measurement, the following relationship is obtained:

$$x_{jk} = (\delta_j/\delta_i)x_{ik} = \kappa_{ji}x_{ik} \quad \text{for } i, j = 1, 2, 3 \text{ and } k = 1, \ldots, N \quad (10)$$

Substituting Eq. (10) into Eq. (5), the covariance of points M_i and M_j can be calculated as:

$$\sigma_{ij} = 1/(N-1)\sum_{k=1}^{N}(x_{ik} - \bar{x}_i)(x_{jk} - \bar{x}_j)$$

$$= 1/(N-1)\sum_{k=}^{N}\delta_j/\delta_i(x_{ik} - \bar{x}_i)^2 = \delta_j/\delta_i\sigma_i^2 \quad (11)$$

where $\delta_i = d(\text{CTE}, M_i)$ is the distance between CTE $(=P_1$; Fig. 4) and M_i. From Eq. (4) in Ceglarek and Shi (1996):

$$\sigma_i = [d(\text{CTE}, M_i)/d(\text{TE}, \text{CTE})]\sigma_{\text{TE}}^F \quad (12)$$

Therefore, substituting Eq. (12) to Eq. (11), we obtain Eq. (7). Q.E.D.

Theorem 1 extends the linear relation between variances and the fixture geometry presented in Ceglarek and Shi (1996) into more general relations between elements of the covariance matrix and fixture geometry.

Class of Covariance Matrices Representing Failure of TE. In general, the obtained results allow the creation of a general covariance matrix representing a single TE fault. For example a type-3 fault (failure of P_2; Figs. 1(*a*, *c*) and 3), which corresponds to a fault with one complement tooling element ($n_{\text{CTE}} = 1$) can be derived from Eq. (7) and presented in the following form:

$$\Sigma^o = \frac{(\sigma_{\text{TE}}^F)^2}{g^2}\begin{bmatrix} a^2 & ab & ac & ad & ae & af \\ ab & b^2 & bc & bd & be & bf \\ ac & bc & c^2 & cd & ce & cf \\ ad & bd & cd & d^2 & de & df \\ ae & be & ce & de & e^2 & ef \\ af & bf & cf & df & ef & f^2 \end{bmatrix} \quad (13)$$

where a, b, c, d, e, f, and g can be derived from Eq. (7) (Ceglarek, 1994). The covariance matrix shown in Eq. (13) represents the general class of covariance matrices for any single tooling element fault in the fixture. Eq. (13) is used in the next section to analytically estimate the eigenvector error caused by additive uncorrelated noise.

3.2 Eigenvalue-Eigenvector Pair Error Caused by Additive Uncorrelated Noise. The error of the eigenvalue-eigenvector pair directly reflects the error of the diagnostic vector, since its elements are the elements of the eigenvector. This section analyzes the error of the eigenvector caused by additive uncorrelated noise in two cases: (1) noise with identical variance for each sensor, and (2) nonequal noise variances for each sensor. For these two cases, the eigenvalue-eigenvector pair for data with and without noise is compared.

The eigenvalues $\lambda_1, \lambda_2, \ldots, \lambda_n$ (data with measurement noise) are computed by solving the characteristic polynomial and then compared with the eigenvalues, $\lambda_1^o, \lambda_2^o, \ldots, \lambda_n^o$, computed for the data without noise in the following way (Jolliffe, 1976):

$$[\Sigma^o - \lambda^o\mathbf{I}]\mathbf{a} = 0 \quad [\Sigma - \lambda\mathbf{I}]\mathbf{a} = 0 \quad (14)$$

The above equation was solved by using MAPLE V software package (Char et al., 1991). The result is a sequence of the eigenvalues, their algebraic multiplicity, and the set of basis vectors for the eigenspace corresponding to each eigenvalue. The dominant eigenvector $\mathbf{a}_1$ (or $\mathbf{a}_1^o$) is obtained by solving the following linear systems with and without noise respectively:

$$(a) \quad (\Sigma - \lambda_1\mathbf{I})\mathbf{a}_1 = 0 \quad (b) \quad (\Sigma^o - \lambda_1^o\mathbf{I})\mathbf{a}_1^o = 0, \quad (15)$$

where λ_1 (λ_1^o) is the largest eigenvalue.

In the case of 3-2-1 fixture failure diagnosis, covariance matrices of dimension 6×6 are considered. The size of the matrices was selected to allow for the analysis of measurement data from three sensors each with data in the X and Z axes. Since the measurement data in the Y axis are independent from data in X and Z axis, they can be analyzed separately (Ceglarek and Shi, 1996). The eigenvalues and eigenvectors are calculated for a class of covariance matrices Σ^o [Eq. (13)] derived in *Theorem 1*.

Uncorrelated Noise with Constant Variance for Each Sensor. From Eq. (15*b*):

$$\Sigma^o\mathbf{a}_1^o = \lambda_1^o\mathbf{I}\mathbf{a}_1^o \quad (16)$$

Multiplying Eq. (4) by $\mathbf{a}_1^o$, it is obtained:

$$\Sigma\mathbf{a}_1^o = (\Sigma^o + \sigma_\epsilon^2\mathbf{I})\mathbf{a}_1^o \quad (17)$$

Substituting Eq. (15*b*) to Eq. (17), gives:

$$\Sigma\mathbf{a}_1^o = (\lambda_1^o\mathbf{I} + \sigma_\epsilon^2\mathbf{I})\mathbf{a}_1^o \quad (18)$$

which is equivalent to the equation $(\Sigma - (\lambda_1^o + \sigma_\epsilon^2)\mathbf{I})\mathbf{a}_1^o = 0$, defining the system described by the following eigenvalue-eigenvector pair: $(\lambda_1, \mathbf{a}_1) = ((\lambda_1^o + \sigma_\epsilon^2), \mathbf{a}_1^o)$. Comparing the dominant eigenvalues λ_1^o and λ_1 for data with and without noise respectively, it can be said that $\lambda_1 = \lambda_1^o + \sigma_\epsilon^2$.

Theorem 2. Independent, uncorrelated and additive noise with constant variance for each sensor (1) causes eigenvalue errors equal to the noise variance σ_e^2, i.e.,

$$\lambda_1 = \lambda_1^o + \sigma_e^2 \tag{19}$$

and (2) does not cause error in the eigenvectors:

$$\mathbf{a}_1 = \mathbf{a}_1^o \tag{20}$$

Finally, it can be concluded that diagnosis of the TE failure is not corrupted by uncorrelated additive noise as long as all sensor noises are uncorrelated and have the same variance. This situation usually occurs when using the same type of sensors, with the same number of working hours, on the same maintenance schedule.

For the class of covariance matrices shown in Eq. (13), which represents a generic description of the TE failures in the fixture, numerically dominant eigenvalue-eigenvector pair is as follows:

$$\lambda_1 = a^2 + b^2 + c^2 + d^2 + e^2 + f^2 + \sigma_e^2;$$

$$\mathbf{a}_1 = [a/D \quad b/D \quad c/D \quad d/D \quad e/D \quad f/D]^T \tag{21}$$

where $D = \sqrt{a^2 + b^2 + c^2 + d^2 + e^2 + f^2}$, and σ_e is the standard deviation of the uncorrelated, independent noise with identical variance.

Uncorrelated Noise with Different Variance for Each Sensor. The class of covariance matrices Σ [Eq. (13)] with different standard deviations of noise σ_{e1}, σ_{e2}, σ_{e3} for each sensor respectively can be represented as:

$$\Sigma = \frac{(\sigma_{\mathrm{TE}_i}^F)^2}{g^2}\begin{bmatrix} a^2 + \frac{\sigma_{e1}^2 g^2}{(\sigma_{\mathrm{TE}_i}^F)^2} & ab & ac & ad & ae & af \\ ab & b^2 + \frac{\sigma_{e1}^2 g^2}{(\sigma_{\mathrm{TE}_i}^F)^2} & bc & bd & be & bf \\ ac & bc & c^2 + \frac{\sigma_{e2}^2 g^2}{(\sigma_{\mathrm{TE}_i}^F)^2} & cd & ce & cf \\ ad & bd & cd & d^2 + \frac{\sigma_{e2}^2 g^2}{(\sigma_{\mathrm{TE}_i}^F)^2} & de & df \\ ae & be & ce & de & e^2 + \frac{\sigma_{e3}^2 g^2}{(\sigma_{\mathrm{TE}_i}^F)^2} & ef \\ af & bf & cf & df & ef & f^2 + \frac{\sigma_{e3}^2 g^2}{(\sigma_{\mathrm{TE}_i}^F)^2} \end{bmatrix} \tag{22}$$

where a, b, c, d, e, f, and g are the coefficients of covariance matrices from Eq. (13) representing type-i faults of tooling element (TE_i), for $i = 1, 2, \ldots, 6$. The σ_{e1}^2, σ_{e2}^2, and σ_{e3}^2 represent variances of uncorrelated, independent noise for sensors 1, 2, and 3 (M_1, M_2, and M_3) respectively. The other elements of the matrix Σ are the same as in Eq. (13).

Comparing the dominant eigenvalues λ_1 and λ_1^o for data with and without noise, the nonlinear impact of the noise on the eigenvalues can be seen. Similarly, the relation between the eigenvectors and noise is nonlinear. In general, the eigenvalues can be represented by function ϕ as follows:

$$\lambda_i = \phi(a, b, c, d, e, f, g, \sigma_{e1}, \sigma_{e2}, \sigma_{e3}, \sigma_{\mathrm{TE}}^F) \tag{23}$$

In a similar manner, the eigenvectors can be represented by nonlinear function φ as follows:

$$a_i = \varphi(a, b, c, d, e, f, g, \sigma_{e1}, \sigma_{e2}, \sigma_{e3}, \sigma_{\mathrm{TE}}^F) \tag{24}$$

The detailed expressions of Eqs. (23) and (24) are obtained using MAPLE V and the results are presented in Ceglarek (1994).

The above relations are used in the following section to estimate the error of fixture failure diagnosis.

4 Fixture Failure Diagnosis with Additive Uncorrelated Noise

This section presents the procedure for estimating the maximum noise level, σ_e, which still allows for correct diagnosis of the pre-determined TE faults. The fault diagnosis performance is evaluated by using the coefficient η [Eq. (2)]. This evaluation is based on two criteria and is conducted through a series of simulations.

Criteria: The fixture failure diagnosis procedure assumes that only one major fault occurs in the system (assembly line). The diagnosis procedure is based on the results and conclusions obtained by Ceglarek and Shi (1996), which can be summarized as:

1. Correct fixture failure diagnosis can be realized if $\eta < 40\%$,
2. In the case of type-i fault, eigenvector $\mathbf{a}^o$ computed for data without noise is equal to diagnostic vector $\mathbf{d}(i)$:

$$\mathbf{a}^o = \mathbf{d}(i) \tag{25}$$

For the purpose of this discussion, the coefficient η (Eq. (2)) is modified to the form used during simulations. By substituting Eq. (25) into Eq. (2), we have:

$$\eta = 2\|g_i(\mathbf{a}) - g(\mathbf{d}(i))\| \cdot 100\% = 2\|g_i(\mathbf{a}) - g(\mathbf{a}^o)\| \cdot 100\% \tag{26}$$

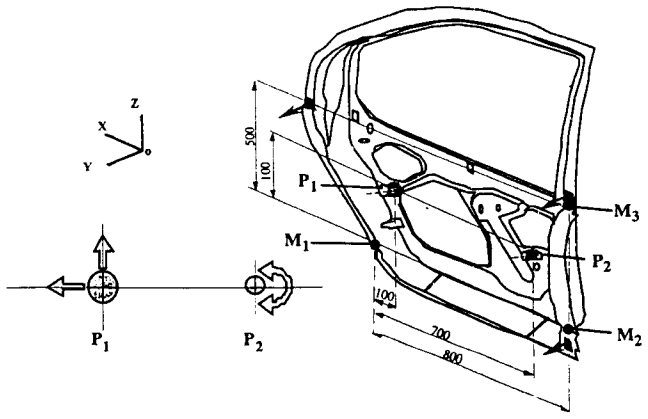

Fig. 5 The geometry of the fixture used for simulations

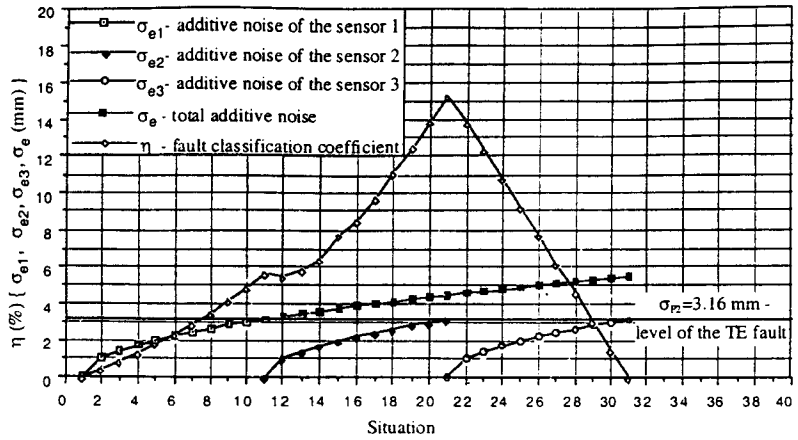

Fig. 6 Impact of the additive uncorrelated noise on the fault classification

Furthermore, by substituting Eq. (1) to Eq. (26), the following can be obtained:

$$\eta = 2\|\mathbf{d}^T(i)\{\mathbf{a} - \mathbf{d}(i)\}\| \cdot 100\% \tag{27}$$

Based on the Cauchy-Schawarz inequality (Strang, 1988), Eq. (27) can be rearranged as:

$$\eta = 2\|\mathbf{d}^T(i)\{\mathbf{a} - \mathbf{d}(i)\}\| \cdot 100\% \le 2\|\mathbf{a} - \mathbf{d}(i)\| \cdot 100\% \tag{28}$$

Thus, finally inserting Eq. (25) to Eq. (28):

$$\eta \le \eta^* := 2\|\mathbf{a} - \mathbf{a}''\| \cdot 100\% \tag{29}$$

where $\mathbf{a}''$ is an eigenvector obtained from diagnostic matrix for a given fault.

Simulations and Case Study. A door inner fixture (locator layout) is shown in Fig. 5. The simulations were conducted for a failure of the locating pin P_2 (Fig. 5). The magnitude of the failure measured by dimensional variation is $\sigma_{P2} = 3.16$ mm. Failure of the locating pin P_2 causes a variation of the whole component registered by sensors M_1, M_2, and M_3. To simulate the real measurements captured by sensors, noise with magnitudes varying from $\sigma_e = 0$ to $\sigma_e = 3.16$ mm was added to the data (sample size of 400). The impact of the noise is shown based on the coefficient η defined in Eq. (29). The simulations were conducted in two steps. The objective of the first step was to estimate the biggest error of the coefficient η for different configurations of the noise levels for each sensor. The second step estimates the error level needed to reach η equal 40% (criterion 1), using the most error-prone configuration.

The results for the first step of the conducted simulations are presented in Fig. 6, which shows simulations for 11 different noise levels for each sensor. The 11 noise levels are simulated in the 31 different configurations for different noises: σ_{e1}, σ_{e2}, and σ_{e3} added to the sensors M_1, M_2, and M_3 respectively. The noise level $\sigma_e = 3.16$ mm is equivalent to the standard deviation of the fault level.

It can be said that the error of the coefficient η mainly depends not on the standard deviation of noise for each sensor, but on the difference between their standard deviations. The biggest error is for $\sigma_{e1} = \sigma_{e2} = 3.16$ mm, and $\sigma_{e3} = 0$, and is equal to $\eta = 15.3\% < \eta_0 = 40\%$ (configuration 21 in Fig. 6).

The second step of the simulation was conducted for the selected configuration 21, $\sigma_{e1} = \sigma_{e2}$, and $\sigma_{e3} = 0$. This is the configuration that is the most sensitive to noise. Based on this configuration, the error as a function of noise level is calculated. The second part of the simulation estimates the maximum noise level for conducting correct fault isolation. Fig. 7 shows the relation between noise level and fault isolation bias coefficient η. In the case of the failure of locating pin P_2, the maximum tolerable noise is estimated as $\sigma_{e1} = \sigma_{e2} = 5.48$ mm (total noise $\sigma_e = 7.75$ mm), which is equal to 173.4% of the fault variation level.

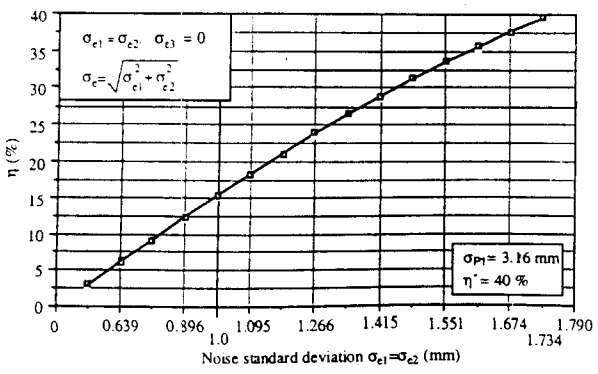

Fig. 7 The relation between η and total noise standard deviation σ_e

5 Conclusions and Summary

The assembly line is prone to failure because of its complexity, high production levels, and rapidly changing requirements of the assembly process. Preventing these failures from propagating in finished assemblies requires continuous fault detection of tooling equipment—fixture failure diagnosis.

This paper expands earlier developed assembly fixture fault diagnosis methodology (Ceglarek and Shi, 1996) by considering the impact of measurement noise on the diagnostic results. The proposed solution provides a new analytical tool to address the diagnosability issue during the assembly process design stage. An evaluation of fault diagnosis index as a function of noise, fixture geometry, and sensor location is presented. The index is derived from the general class of covariance matrices describing tooling faults.

Based on the analytical results, simulation studies were conducted to estimate the maximum allowable additive uncorrelated noise level. Our analysis showed that the impact of noise depends not only on the noise level, but also on the differences between noise levels for different sensors. We point out that uncorrelated additive noises with identical variances for each sensor do not influence the elements of the diagnostic vector. Based on the worst configuration of the noise magnitude between sensors, we estimate that tooling faults can still be accurately isolated if noise standard deviation does not exceed 173% of the fault magnitude standard deviation.

References

Anderson, T. W., 1965, *An Introduction to Multivariate Statistical Analysis*, John Wiley and Sons, Inc., New York, NY.

Ceglarek, D., 1994, *Knowledge-Based Diagnosis for Automotive Body Assembly: Methodology and Implementation*, Ph.D. Dissertation, Univ. of Michigan, Ann Arbor.

Ceglarek, D., Shi, J., and Wu, S. M., 1994, "A Knowledge-based Diagnosis Approach for the Launch of the Auto-body Assembly Process," ASME JOURNAL OF ENGINEERING FOR INDUSTRY, Vol. 116, No. 4, pp. 491–499.

Ceglarek, D., and Shi, J., 1995, "Dimensional Variation Reduction for Automotive Body Assembly," *Manufacturing Review*, Vol. 8, No. 2, pp. 139–154.

Ceglarek, D., and Shi, J., 1996, "Fixture Failure Diagnosis for the Autobody Assembly Using Pattern Recognition," ASME JOURNAL OF ENGINEERING FOR INDUSTRY, Vol. 118, No. 1, pp. 55–66.

Char, B. W., Geddes, K. O., Gonnet, G. H., Leong, B. L., Monagan, M. B., and Watt, S. W., 1991, *Maple V Library Reference Manual*, Springer-Verlag, New York, NY.

Chou, Y-C., Chandru, V., and Barash, M. M., 1989, "A Mathematical Approach to Automatic Configuration of Machining Fixtures: Analysis and Synthesis," ASME JOURNAL OF ENGINEERING FOR INDUSTRY, Vol. 111, pp. 299–306.

Down, M. H., Lowe, V. W., and Daugherty, B. R., 1995, "Measurement System Analysis—Reference Manual," The American Society for Quality Control (ASQC) and The Automotive Industry Action Group (AIAG).

Grubbs, F. E., 1948, "On Estimating Precision of Measuring Instruments and Product Variability," *Journal of American Statistical Association*, Vol. 43, pp. 243–264.

Hu, S., and Wu, S. M., 1992, "Identifying Root Causes of Variation in Automobile Body Assembly Using Principal Component Analysis," *Trans. of NAMRI*, Vol. 20, pp. 311–316.

Jolliffe, I. T., 1986, *Principal Component Analysis*, Springer-Verlag, New York, NY.

Schwarz, S. A., and Lu, S. C-Y., 1992, "Representation, Acquisition, and Manipulation of Probabilistic Attribute Values to Support Engineering Decision Making," *Trans. of NAMRI*, Vol. 20, pp. 261–267.

Strang, G., 1988, *Linear Algebra and its Application*, Harcourt Brace Jovanovich, Inc., San Diego, CA.

Thompson, W. A., 1963, "Precision of Simultaneous Measurement Procedures," *Journal of American Statistical Association*, Vol. 58, pp. 474–479.

Tlusty, J., and Andrews, G. C., 1983, "A Critical Review of Sensors for Unmanned Machining," *Annals of the CIRP*, Vol. 32, pp. 563–572.